



H₂O Emission in Ultra-Luminous Infrared Galaxies at $z \sim 2-4$

Chentao Yang^{1,2,3}, Alain Omont^{2,4}, Alexandre Beelen³, Eduardo González-Alfonso⁵ and Yu Gao¹ on behalf of *Herschel*-ATLAS* and IRAM Teams

1. Purple Mountain Observatory; 2. Institut d'Astrophysique de Paris, CNRS; 3. Institut d'Astrophysique Spatiale; 4. UPMC Univ. Paris 06; 5. Universidad de Alcalá



Abstract

Herschel observations of local infrared bright galaxies have revealed a rich spectrum of submillimeter H₂O rotational emission lines up to upper level energy of $E_U/k = 642$ K. H₂O is found to be the second strongest molecular emitter after CO in the submillimeter band, sometimes with comparable intensity. The strong H₂O lines provide a unique diagnostic for a totally different regime than the CO usual lines considering its very different excitation process. Using IRAM PdBI, we have extended our H₂O detections with 15 more lines in 11 high- z lensed Ultra-Luminous Infrared Galaxies (ULIRGs, five of them have both para $J=2$ and ortho $J=3$ H₂O detected) discovered by *H*-ATLAS. The total number of the H₂O detected galaxies in our sample is now 17. As in the local ULIRGs, the intensity of the high- z H₂O lines are strong, ≥ 0.5 of the mid- J CO lines. The CO detected using IRAM 30m telescope in some of the sources have similar line profiles as H₂O, indicating their similar spatial distributions considering the differential lensing. The intrinsic H₂O line luminosity L_{H_2O} increases slightly faster than linearly with the intrinsic infrared (IR) luminosity, $\propto L_{IR}^{1.1-1.2}$, for the $J=2$ ($E_U/k \sim 100$ K) and $J=3$ ($E_U/k \sim 300$ K) H₂O lines. This implies that IR pumping is important for the H₂O excitation in these sources. Also, the ratio H₂O $J=2/J=3$ varies in those high- z ULIRGs, likely reflecting different physical conditions, e.g., dust temperature and far-IR opacity. Besides H₂O, we have also detected H₂O⁺ and H₂¹⁸O in some of the galaxies. The intensity ratios together with the isotopic ratio suggest that the H₂O lines are well saturated while the H₂O⁺ and H₂¹⁸O lines are likely to be optically thin. However, high resolution study is still needed for revealing the spatial distribution of H₂O emission within.

Sample selection and observation

How to observe H₂O?

- Local universe: space telescopes like *Herschel* (See our poster **S315p.186** for a local survey)
- Redshifted (high- z) line observation with high sensitivity: **gravitational lensing!**
- Source selection:
 - Select the bright **lensed** ULIRGs from *H*-ATLAS catalog.
 - The redshifts are secured by the previous CO detections via CARMA (Riechers et al. in prep.), GBT (Harris et al. 2012; Lupu et al. 2012) and PdBI (Krips et al. in prep.). The redshift distribution is shown in Fig. 1.
 - Lensing properties are well described in Bussmann et al. (2013).
- The chosen sources (**17 in total**) and H₂O lines (as shown in Fig. 2):
 - Sources with both **para $J=2$** and **ortho $J=3$ H₂O** lines observed:
 - GAMA field sources: *G09v1.97*, *G12v2.43*
 - Northern Galactic Pole field sources: *NBv1.78* ($J=3$ H₂O only) *NCv1.143*, *NAv1.195*, *GAv1.177*

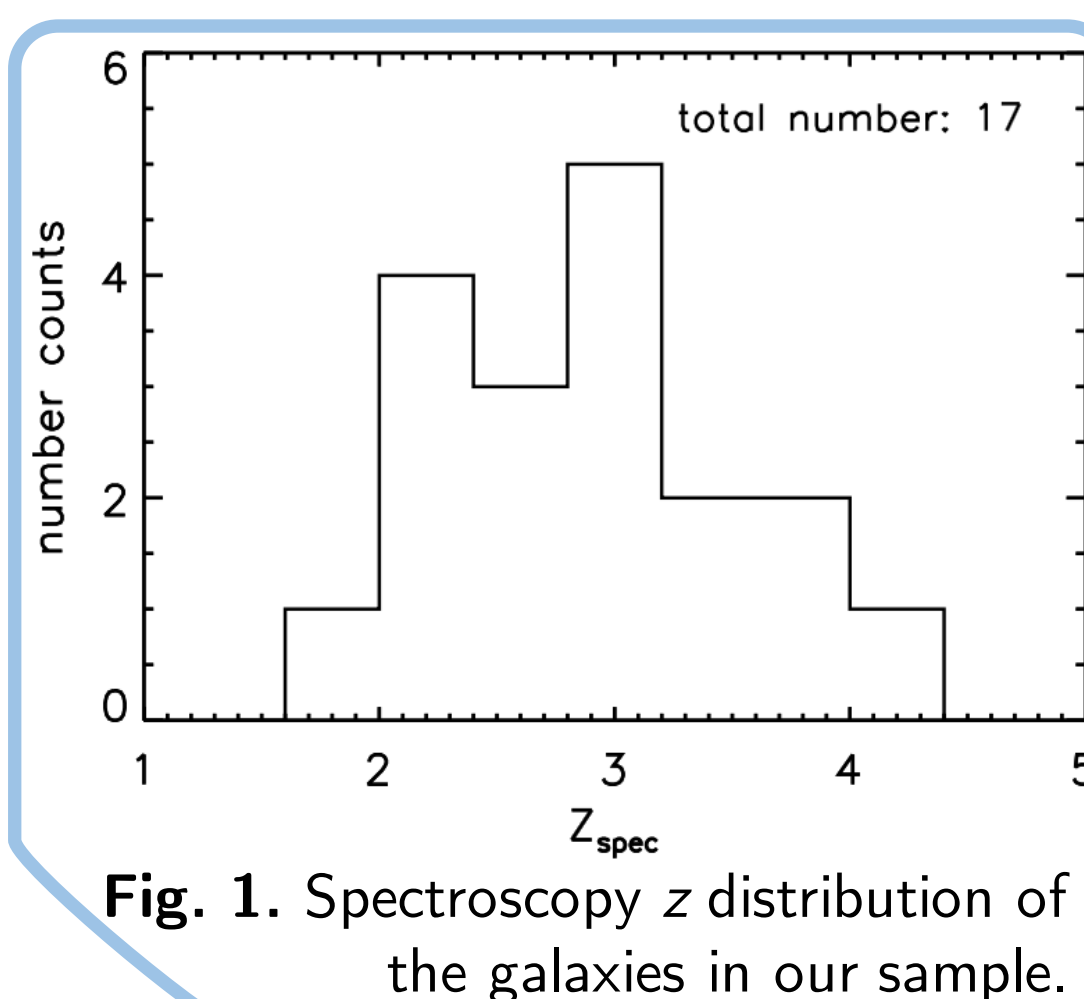


Fig. 1. Spectroscopy z distribution of the galaxies in our sample.

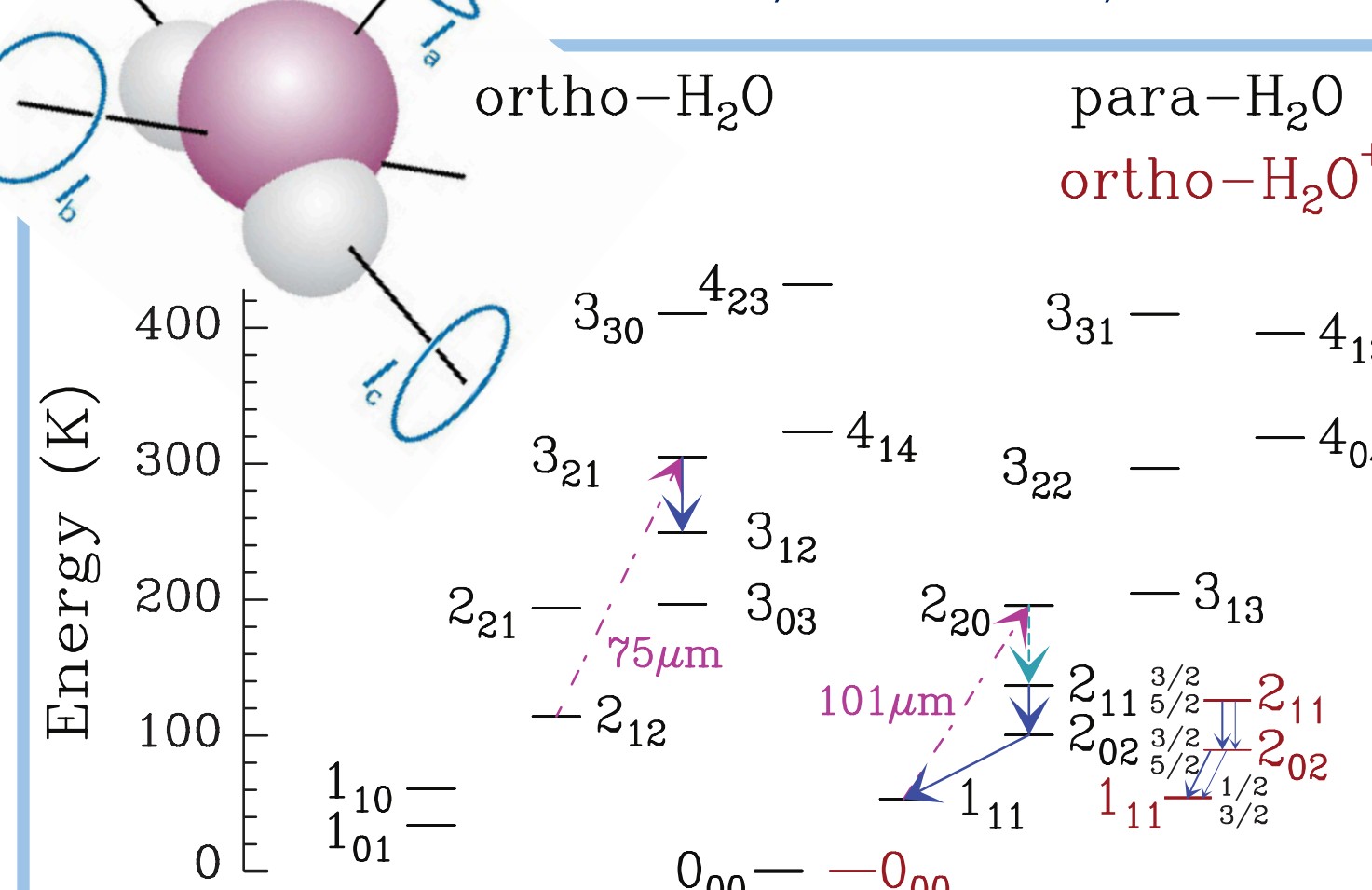


Fig. 2. H₂O and H₂O⁺ energy level diagram shown in black and red color, respectively. Blue arrows are the H₂O emission lines we have observed in this work. Pink dashed lines show the H₂O IR pumping paths in our model, with the labeled wavelength.

- Sources with only **para $J=2$ H₂O** observed:
 - Science Demonstration Phase filed: *SDP11*
 - NCv1.268*, *NAv1.56*
 - G09v1.124*, *G09v1.40*
- Previous detected sources in Omont et al. (2013):
 - SDP81*, *SDP9*, *SDP17b*
 - G12v2.30*, *G15v2.779*
 - NAv1.144*, *NBv1.78* ($J=2$)
- Additional observations:
 - CO lines via IRAM 30m
 - Dense gas via PdBI

Results

- H₂O emission line is strong:** we have robustly detected **almost all** the H₂O lines with high signal to noise ratios. However, the non-detections are H₂O($2_{11}-2_{02}$) in *G09v1.124* and H₂O($3_{21}-3_{12}$) in *NAv1.195*. Our sources represent **close to 80%** of the current high- z detections of the submillimeter H₂O emission.
- As an example,** the images of the H₂O lines and the underlying dust continuum emissions from one of the 17 sources, *NBv1.78*, are shown in Fig. 3. And Fig. 4 shows its H₂O spectra together with the CO lines.

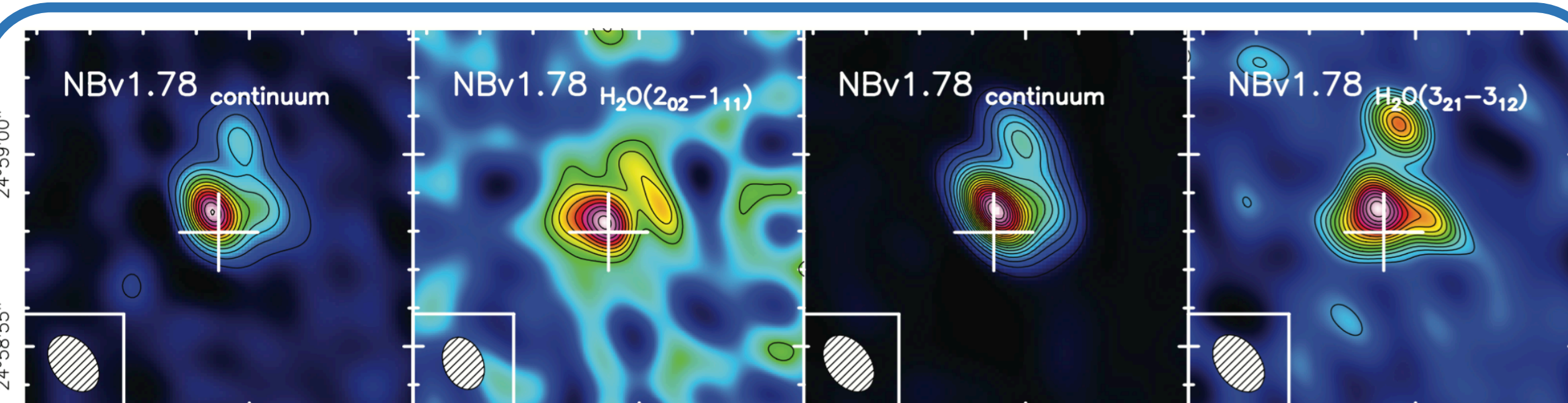
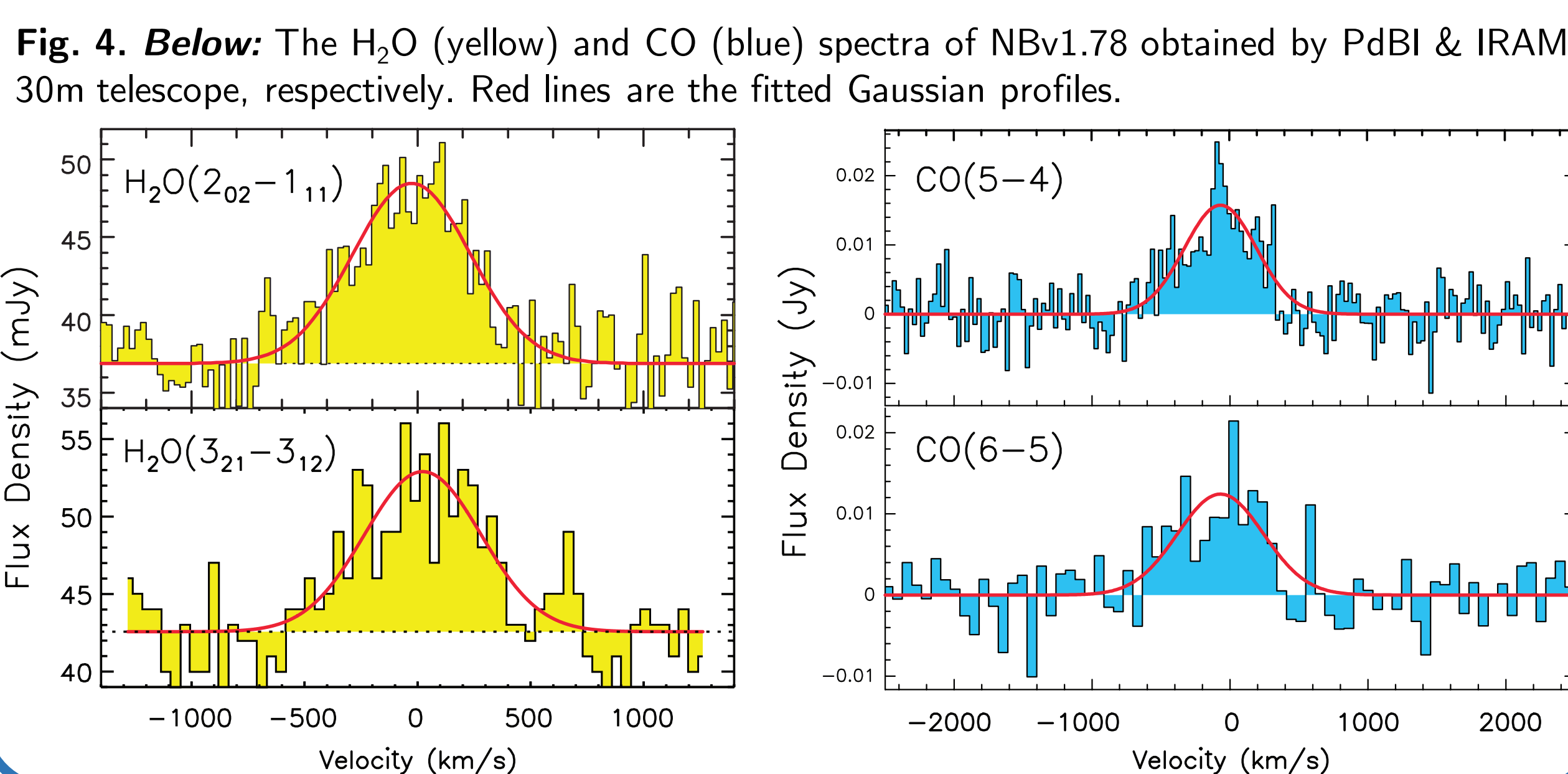


Fig. 3. **Above:** Images of the H₂O emission and the corresponding continuum emission in *NBv1.78*. The contours of the continuum start from 6σ in step of 10σ . And for the H₂O lines, they start from 3σ in step of 1σ . The 1σ contour for the continuum (mJy/beam) and H₂O emission (Jy km s⁻¹/beam) in *NBv1.78* are as follows: H₂O($2_{02}-1_{11}$) (0.28/0.30), H₂O($3_{21}-3_{12}$) (0.21/0.29).



- The H₂O emission has **similar spatial distribution** as the dust emission, especially for the higher- J H₂O lines, being consistent with IR pumping.
- Comparing with mid- J CO lines, the H₂O lines **have similar line profiles**. Thus, they are likely **tracing similar gas structures**.
- We find the H₂O and IR luminosity **are roughly proportional** (Fig. 5).
- Submillimeter H₂O excitation is **dominated by IR pumping**. Therefore, unlike CO rotational lines, it is a **unique diagnostic of strong local far-IR radiation field**.

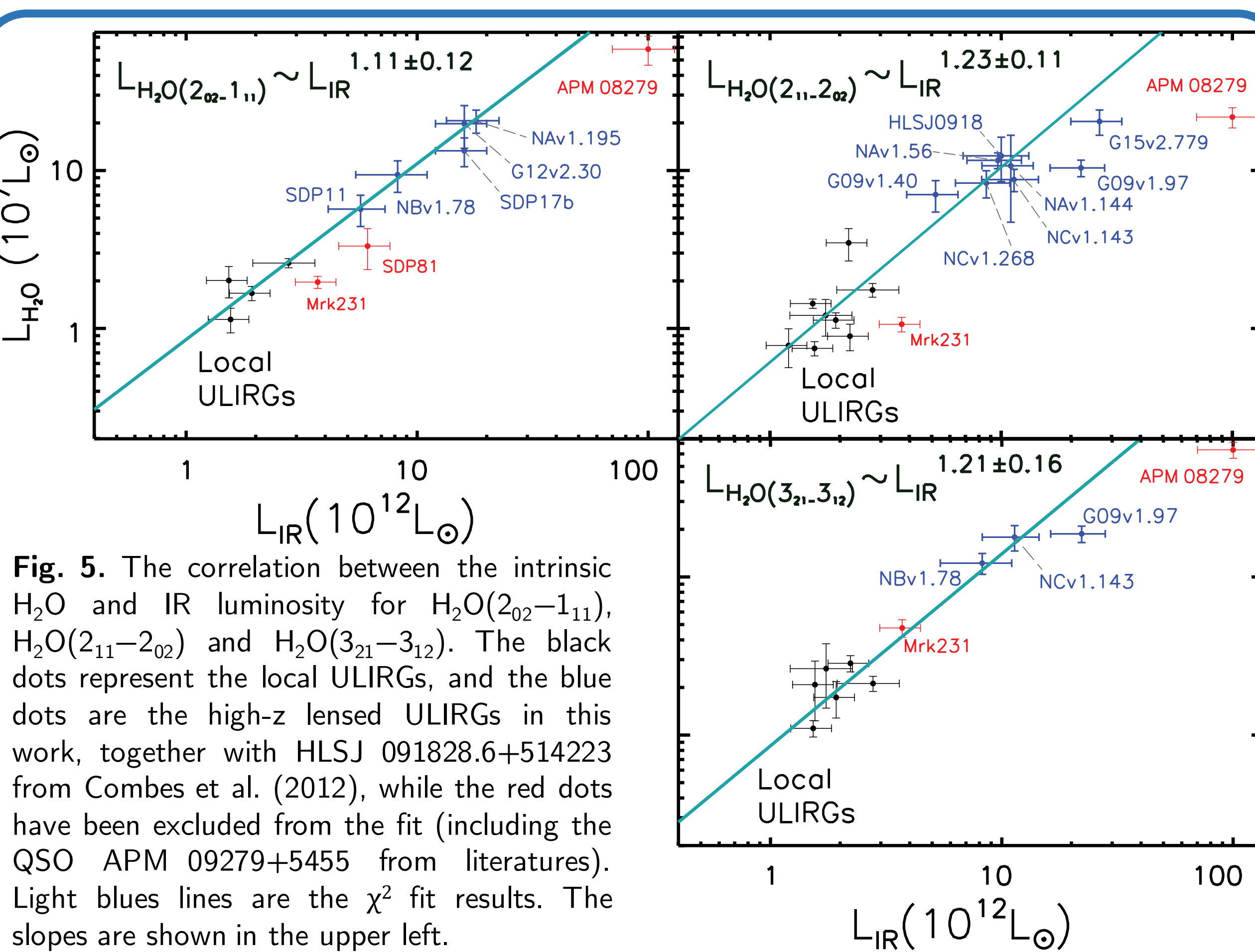


Fig. 5. The correlation between the intrinsic H₂O and IR luminosity for H₂O($2_{02}-1_{11}$), H₂O($2_{11}-2_{02}$) and H₂O($3_{21}-3_{12}$). The black dots represent the local ULIRGs, and the blue dots are the high- z lensed ULIRGs in this work, together with *HLSJ 091828.6+514223* from Combes et al. (2012), while the red dots have been excluded from the fit (including the QSO APM 09279+5455 from literatures). Light blue lines are the χ^2 fit results. The slopes are shown in the upper left.

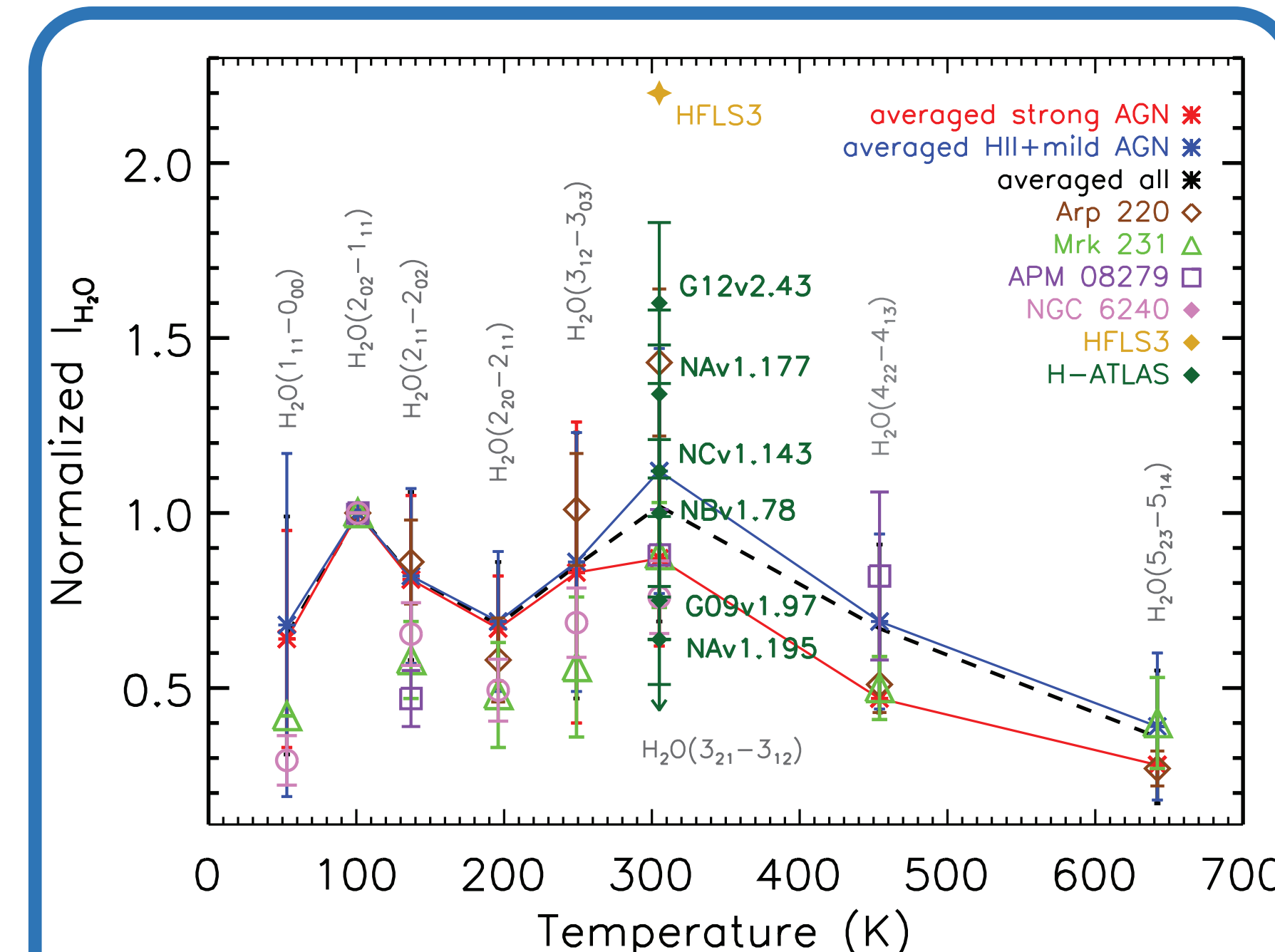


Fig. 6. The H₂O intensities (Jy km s⁻¹) distribution normalized by ($2_{02}-1_{11}$) developed from Yang et al. (2013). Dash lines represent the averaged ratios of the local galaxies. Dark green diamonds are the high- z lensed galaxies from this work. And *HFLS3* is a unlensed high- z galaxy from Riechers et al. (2013).

H₂O SLED

The ratio $(3_{21}-3_{12})/(2_{02}-1_{11})$ **varies in a large range:** from <0.67 in *NAv1.195* up to 2.2 in *HFLS3*. This difference may represent their intrinsic different physical condition of the local IR radiation fields, if differential lensing is negligible. With a careful H₂O excitation modelling (using the method

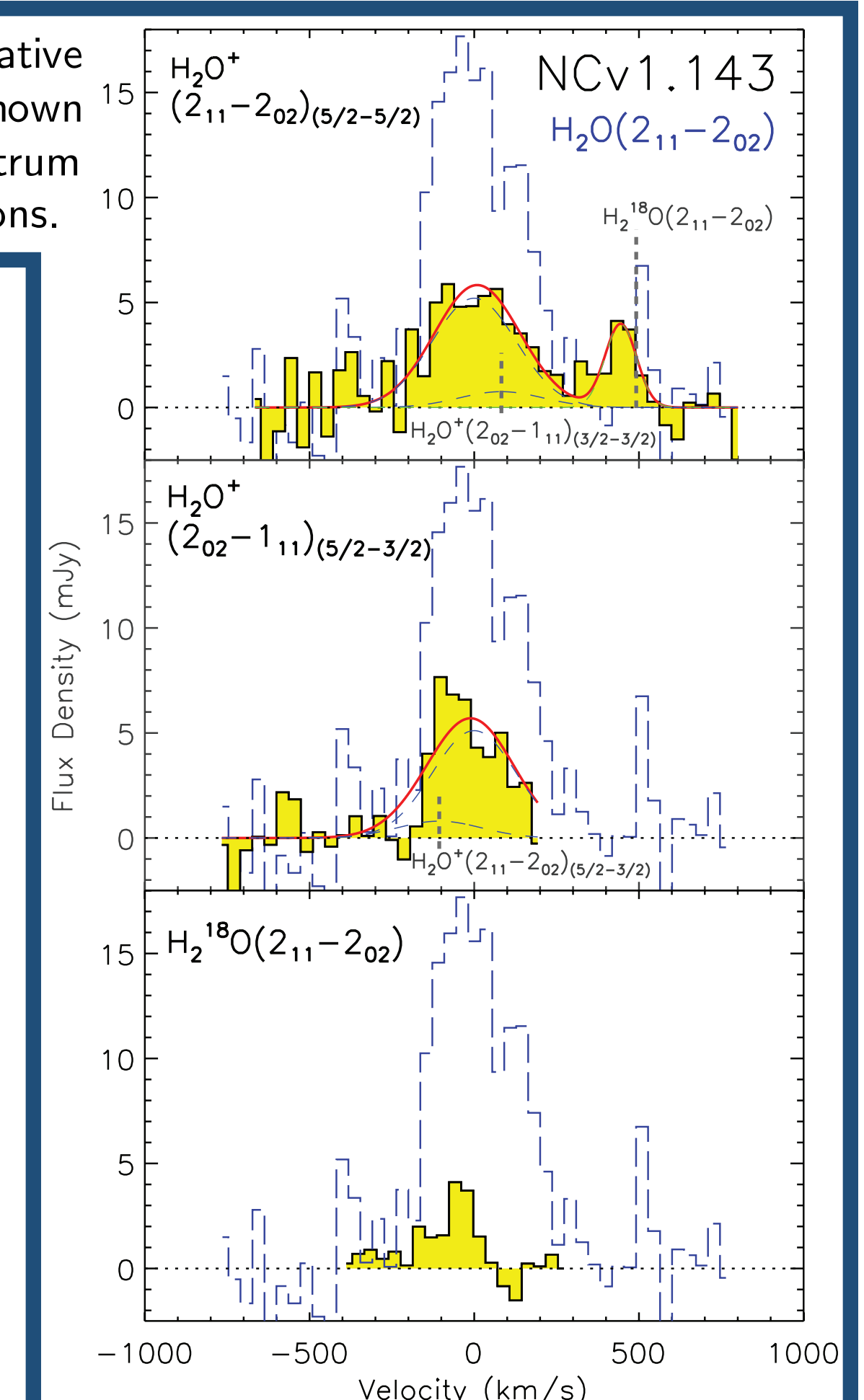
from G-A14) for 5 sources with both $J=2$ & $J=3$ lines detected, we find that **their intensity ratio is sensitive to the dust temperature and continuum opacity in the far-IR**. However, more transitions are needed for better constrains on opacity and H₂O column density.

Detection of H₂O⁺ lines

Fig. 7. The detections of H₂O⁺ and the tentative detection of H₂¹⁸O emission in *NCv1.143* as shown by the yellow spectra in each panel. H₂O spectrum has been overlaid on each spectrum as comparisons.

First detections of H₂O⁺ emission in the high- z lensed galaxies:

- We have detect H₂O⁺($2_{11}-2_{02}$) $J_{5/2-5/2}$ in *NCv1.143* (Fig. 7) and *G15v2.779*; and ($2_{02}-2_{11}$) $J_{5/2-3/2}$ in *NCv1.143* (Fig. 7) and *G09v1.97*.
- Tentative detection of $J=2$ H₂¹⁸O (Fig. 7, bottom panel) needs to be confirmed with more sensitive observation.
- Analysis of the line ratios among H₂O, H₂O⁺ and H₂¹⁸O, together with the abundance ratios suggests that **H₂O are well saturated while the H₂O⁺ & H₂¹⁸O are likely to be optically thin**.



Prospect

- H₂O is strong and suitable for systematic high- z studies using the current facilities like PdBI and ALMA.
- By combining the analysis of CO lines (our ongoing project), we will have a fully view of the physical condition of the molecular gas, helping us to study varies processes in ISM of the very early universe.
- ALMA can easily detect H₂O⁺ and H₂¹⁸O lines, which are important for both dynamical analysis and astrochemistry studies at high- z .

References

- Bussmann, R. S., Pérez-Fournon, I., Amber, S., et al. 2013, *ApJ*, 779, 25
- Combes, F., Rex, M., Rawle, T. D., et al. 2012, *A&A*, 538, L4
- González-Alfonso, E., Fischer, J., Aalto, S., & Falstad, N. 2014, *A&A*, 567, A91 (G-A14)
- Harris, A. I., Baker, A. J., Frayer, D. T., et al. 2012, *ApJ*, 752, 152
- Lupu, R. E., Scott, K. S., Aguirre, J. E., et al. 2012, *ApJ*, 757, 135
- Omont, A., Yang, C., Cox, P., et al. 2013, *A&A*, 551, A115
- Riechers, D. A., Bradford, C. M., Clements, D. L., et al. 2013, *Nature*, 496, 329
- Yang, C., Gao, Y., Omont, A., et al. 2013, *ApJ*, 771, L24

*: *Herschel* -Astrophysical Terahertz Large-Area Survey: Eales, S., Dunne, L., et al. 2010, *PASP*, 122, 499

